BIOLOGY OF REPRODUCTION (2016) **94**(5):109, 1–10
Published online before print 16 March 2016.
DOI 10.1095/biolreprod.115.134981

Knockdown of Progesterone Receptor (PGR) in Macaque Granulosa Cells Disrupts Ovulation and Progesterone Production[1]

Cecily V. Bishop,[2,3] Jon D. Hennebold,[3,5] Christoph A. Kahl,[4] and Richard L. Stouffer[3,5]

[3]*Division of Reproductive & Developmental Sciences, Oregon National Primate Research Center, Beaverton, Oregon*
[4]*Molecular Virology Support Core, Oregon National Primate Research Center, Beaverton, Oregon*
[5]*Department of Obstetrics and Gynecology, Oregon Health & Science University, Portland, Oregon*

ABSTRACT

Adenoviral vectors (vectors) expressing short-hairpin RNAs complementary to macaque nuclear progesterone (P) receptor *PGR* mRNA (shPGR) or a nontargeting scrambled control (shScram) were used to determine the role PGR plays in ovulation/luteinization in rhesus monkeys. Nonluteinized granulosa cells collected from monkeys (n = 4) undergoing controlled ovarian stimulation protocols were exposed to either shPGR, shScram, or no virus for 24 h; human chorionic gonadotropin (hCG) was then added to half of the wells to induce luteinization (luteinized granulosa cells [LGCs]; n = 4–6 wells/treatment/monkey). Cells/media were collected 48, 72, and 120 h postvector for evaluation of *PGR* mRNA and P levels. Addition of hCG increased ($P < 0.05$) *PGR* mRNA and medium P levels in controls. However, a time-dependent decline ($P < 0.05$) in *PGR* mRNA and P occurred in shPGR vector groups. Injection of shPGR, but not shScram, vector into the preovulatory follicle 20 h before hCG administration during controlled ovulation protocols prevented follicle rupture in five of six monkeys as determined by laparoscopic evaluation, with a trapped oocyte confirmed in three of four follicles of excised ovaries. Injection of shPGR also prevented the rise in serum P levels following the hCG bolus compared to shScram ($P < 0.05$). Nuclear PGR immunostaining was undetectable in granulosa cells from shPGR-injected follicles, compared to intense staining in shScram controls. Thus, the nuclear PGR appears to mediate P action in the dominant follicle promoting ovulation in primates. In vitro and in vivo effects of PGR knockdown in LGCs also support the hypothesis that P enhances its own synthesis in the primate corpus luteum by promoting luteinization.

luteinization, ovulation, PGR, progesterone, shRNA, siRNA

INTRODUCTION

Factors contributing to ovulation and luteinization of the dominant follicle in primates are of intense research interest for development of both novel contraceptives and infertility treatments. During the menstrual cycle, the midcycle surge of luteinizing hormone (LH) induces a cascade of events culminating in ovulation of the single dominant follicle [1]. Also, the theca and granulosa cells of the ovulatory/luteinizing follicle switch steroid production from androgen/estrogen (estradiol [E2]) to predominantly progesterone (P), with lesser E2 synthesis [2]. In addition to critical endocrine functions, e.g., in the uterus for implantation, these steroids have local actions within the follicle/corpus luteum (CL) itself. The nuclear estrogen receptor, as well as androgen receptor and the nuclear P receptor (PGR), are expressed within the ovulatory, luteinizing follicle in primates [3], whereas the nonclassical P receptor, P receptor membrane component 1 (PGRMC1), is reportedly present in luteinized granulosa cells (LGCs) of periovulatory follicles of women [4]. When rhesus macaques were treated with trilostane (TRL), a compound that prevents 3β-hydroxysteroid dehydrogenase (HSD3B2) from converting pregnenolone to P, periovulatory processes were disrupted during controlled ovarian stimulation (COS) protocols [5]. The ovaries had numerous unruptured follicles, and very few oocytes were recovered from the oviducts. Moreover, circulating P levels were diminished in the luteal phase compared to controls. Notably, P replacement by concurrent administration of R5020 (a synthetic progestin) restored ovulation, whereas dihydrotestosterone (DHT) administration did not, supporting the hypothesis that P-receptor signaling is critical for periovulatory events in primates. However, these pharmacologic studies were limited by the fact that TRL also interferes with production of estrogens and androgens in addition to P, plus the specific roles of the nuclear and membrane P receptor in the primate follicle could not be distinguished.

The most studied P receptor to date is the nuclear PGR. A single gene encodes both the A and B isoforms of *PGR* mRNA; *PR-B* is the longer, full-length isoform whereas *PR-A* is truncated, lacking 164 amino acids at the N-terminal domain [6]. Both receptor isoforms translocate to the nucleus upon ligand binding and regulate gene transcription. The female *Pgr* double-knockout (both *Pgr-a* and *Pgr-b*; PRKO) mouse is sterile: its ovaries have large antral follicles that fail to initiate ovulation and oocyte expulsion [7], but appear to luteinize [8]. Although evidence gathered from studies performed in PRKO mice suggests a critical role for PGR during ovulation, rodents and primates differ in ovarian physiology (i.e., single ovulatory follicle vs. multiple ovulatory follicles) and in follicular PGR protein expression [9]. Also, the interval from the onset of the LH surge to ovulation is much longer, and the cascade of events leading to oocyte expulsion and luteinization differs somewhat in primates compared to rodents [10]. Moreover, rodents do not develop functional CLs unless pregnancy or pseudopregnancy occurs, whereas one CL develops in primates in response to the LH surge during the menstrual cycle. Therefore, *PGR* gene knockdown studies performed in a

[1]Supported by NIH R01HD020869 (R.L.S.) and P51OD011092 (support for National Primate Research Center). These data were presented at the 70th Annual Meeting of the American Society for Reproductive Medicine, October 2014.
[2]Correspondence: Cecily V. Bishop, Division of Reproductive & Developmental Sciences, Oregon National Primate Research Center, 505 NW 185th Ave., Beaverton, OR 97006. E-mail: bishopc@ohsu.edu

Received: 26 August 2015.
First decision: 7 October 2015.
Accepted: 14 March 2016.

eISSN: 1529-7268 http://www.biolreprod.org
ISSN: 0006-3363

primate model are needed to clarify the role of P signaling via PGR in primate ovulation and luteinization. Recent molecular technologies now allow manipulation of gene expression in cells in vitro and tissues in vivo at precisely timed intervals. The goal of the current study was to employ RNA interference (RNAi) technology (reviewed in [11]) through adenoviral vector (vector) delivery of a short-hairpin RNA (shRNA) sequence that encodes a short interfering RNA (siRNA) capable of silencing *PGR* (A and B) mRNA expression [12]. Optimizing the timing and efficacy of adenoviral delivery of gene-modifying agents to granulosa cells of the dominant follicle of rhesus monkeys in vitro and in vivo was performed prior to evaluating the periovulatory effects of *PGR* mRNA knockdown.

MATERIALS AND METHODS

Animals

All experiments involving rhesus females were performed with approval of the Oregon Health & Science University Institutional Animal Care and Use Committee at the Oregon National Primate Research Center (ONPRC), in accordance with the National Institutes of Health Guide for the Care and Use of Laboratory Animals. Rhesus monkeys were cared for by the ONPRC Division of Comparative Medicine (DCM) as previously reported [13]. All surgical procedures were performed by the veterinary staff of the ONPRC DCM Surgical Services Unit (SSU).

RNA Interference

A specific silencing siRNA complementary to the rhesus macaque (*Macaca mulatta*) *PGR* gene (NCBI gene ID 613024), targeting both P receptor transcript variant 1/isoform 1 (NCBI reference sequence NM_001278456.1, also known as *PR-B*) and variant 2/isoform 2 (NCBI reference sequence NM_001278457.1, also known as *PR-A*), was designed using BLOCK-iT RNAi Designer (Life Technologies, Grand Island, NY; siPGR, Supplemental Table S1). A scrambled siRNA was designed to serve as a nontargeting control (siScram). Sequences were encoded within Stealth RNAi siRNAs (Life Technologies) and evaluated for their ability to deplete *PGR* mRNA and protein expression in the macaque mammary fibroblast cell line CMMT (obtained from American Type Culture Collection [ATCC]; ATCC CRL-6299). Cells were cultured as recommended by ATCC except for use of 10% charcoal-treated fetal calf serum (Valley Biomedical Products and Services Inc.). The targeting siRNA (siPGR), but not the scrambled control siRNA (siScram), suppressed *PGR* mRNA levels without any remarkable off-target effects on related mRNA levels (e.g., *PGRMC1*) or cellular viability/total RNA recovered (data not shown). The siRNA sequences were then expanded into longer shRNAs that included either the *PGR* siRNA or scrambled control sequences (Supplemental Table S1). The shRNAs were cloned into a BLOCK-iT pENTR/U6 entry vector plasmid (Life Technologies) for incorporation into the vectors by the ONPRC Molecular Virology Support Core.

Adenovirus Generation

Vectors expressing shRNA targeting rhesus *PGR* mRNA (shPGR), scrambled shRNA (shScram), or the gene encoding enhanced GFP (*EGFP*) via cytomegalovirus promotor (CMV) were constructed using the ViraPower system (Life Technologies). Briefly, the nucleotide expression cassette (encoding either shRNA or *EGFP*) was transferred from the pENTR/U6 entry plasmid to the adenoviral destination plasmid (pAd/BLOCK-iT) via Gateway recombination. The resulting adenoviral plasmids were then transfected into 293A cells (Life Technologies) to generate recombinant vectors. For production, viruses were expanded and harvested from cells by triple freeze-thaw method. Cell lysates were treated with Benzonase nuclease (Sigma-Aldrich) to digest genomic DNA and virions were purified by iodixanol gradient ultracentrifugation [14] using OptiPrep medium (Sigma-Aldrich). The 25%-40% iodixanol interfaces containing adenovirus were aspirated and buffer exchanged into PBS + 5% glycerol using Amicon Ultra-15 Centrifugal Filter Units (EMD Millipore). To assess biological activity, virus preparations were titered by TCID50 assay on 293A cells, and values were converted to plaque-forming units (pfu). The absence of replication-competent adenovirus was verified using an agarose gel overlay method on A549 indicator cells [15].

Adenovirus Validation

First, the *EGFP* gene-expressing vector was used to determine the optimal viral titer to sufficiently transduce macaque granulosa cells in vitro and in vivo, and to ensure high EGFP expression and low toxicity (by decreased numbers of cells compared to no-virus controls).

Pilot studies were performed on granulosa cells obtained from COS protocols either 36 h following a human chorionic gonadotropin (hCG) bolus as previously described (in vivo LGCs [16]), or prior to the hCG bolus as described below in experiment 1 (nonluteinized granulosa cells [NLGCs]). Granulosa cells were isolated from follicular aspirates and cultured as previously reported [17] on fibronectin-coated 96-well culture plates (BD Biosciences) in DMEM/F12 medium containing 15 mM HEPES, 100 U penicillin/100 μg/ml streptomycin, insulin/transferrin/sodium selenite (ITS) liquid media supplement (Sigma-Aldrich), 0.028 mg/ml LDL (Biomedical Technologies, Alfa Aesar), 0.002 mg/ml aprotinin (Sigma-Aldrich), and 2.5 ng/ml human follicle-stimulating hormone (Organon) in a humidified incubator at 37°C/5% CO_2. For in vivo LGCs, addition of hCG (20 IU/ml; EMD Serono) occurred at the time of plating. Half of the wells containing NLGCs received hCG 24 h after plating to induce in vitro luteinization. As an additional control, CMMT cells (ATCC) were cultured as described above for transduction experiments. All cells were exposed to EGFP vector (range 3.9×10^8–3.9×10^6 pfu/ml). Expression of EGFP transgene was visualized by fluorescence microscopy as described below after 24 h of viral exposure. Cultures were extended for 1 wk to determine toxic effects of adenovirus exposure on granulosa cells, with medium changes occurring every other day.

Next, *EGFP* gene vector was prepared at various titers in vehicle (PBS) for injection into the preovulatory follicle during controlled ovulation (COv) protocols by SSU staff using previously reported methods [18]. The vector was diluted in 50 μl of vehicle and drawn into a tuberculin (1 ml) syringe. The needle was inserted through the wall at the base of the large dominant antral follicle through the stroma of the ovary. Then, 50 μl of follicular fluid was aspirated into the syringe, mixing with the vector solution. After 50 μl of follicular fluid/vector was reinjected into the follicle, the needle was removed and the follicle was observed to ensure leakage and follicle deflation did not occur. Based on previous studies, the macaque dominant follicle contains approximately 200 μl of follicular fluid at this time [18]; therefore, a dilution factor of 1:4 was applied to estimate the final dose delivered (range: 3.9×10^8–3.9×10^7 pfu/ml). Injected ovaries were surgically removed 24 (n = 3) or 72 (n = 3) h postinjection. Ovaries were placed in ice-cold PBS and immediately imaged with an Olympus Inverted System microscope (IX71) attached to a reflected light fluorescence laser with filter to identify fluorescein isothiocyanate (FITC) emission spectra; images were obtained with an Olympic Microfire Camera [19]. Ovaries were also imaged after bisection, and underwent fixation in 4% neutral-buffered formalin at 4°C for 24 h before dehydration in ethanol and paraffin embedding as previously described [19].

Fixed, paraffin-embedded ovaries were cut into 5-μm sections and placed on glass permafrost slides for immunohistochemical visualization of EGFP protein. Several ovarian sections were processed for hematoxylin and eosin staining using established methods [19] to define tissue morphology. Additional slides containing ovarian sections from *EGFP* vector-exposed ovaries (four sections/slide) and archived slides containing macaque ovarian sections obtained 70 h post-hCG administration following COv protocols (four sections/slide) were subjected to citric buffer heat-based antigen retrieval [19] and incubated for 1 h at room temperature in PBS containing 5% normal rhesus monkey serum and 1% bovine serum albumin (BSA). Slides were then incubated overnight with rabbit anti-EGFP antibody (recognizes both wild-type GFP and EGFP; ab290, Abcam) diluted 1:500 in PBS containing 1% BSA. Staining for EGFP protein was visualized with 1 h incubation of alkaline phosphate-conjugated secondary antibody [19], and detected with application of NBT/BCIP substrate (Roche). All sections were processed in the same reaction, and tissue morphology was visualized by nuclear fast-red counterstain (Sigma-Aldrich).

Experiment 1

NLGCs were collected from female monkeys (n = 4) undergoing COS cycles to induce multifollicular development prior to an ovulatory stimulus. Briefly, females were monitored daily for onset of menstruation, and within the first 3 days were placed on an injection regimen consisting of 6 days of recombinant human FSH (30 IU, i.m.) at 0800 and 1600 h, followed by 1 day of FSH:recombinant human LH (30 IU each, i.m.) at 0800 and 1600 h with the GnRH antagonist acyline (75 μg/kg, s.c.) at 0800 h. The following morning, follicular contents were aspirated by laparoscopic techniques [20] to retrieve immature germinal vesicle (GV)-stage cumulus oocyte complexes and NLGCs. Aspirates from individual females were prepared for separate experiments.

Oocytes were removed from the follicular aspirates, and remaining cells were pelleted by centrifugation at 170 × *g* (4°C). Pelleted cells were resuspended in Ham F10 medium containing 25 mM HEPES and 0.1% BSA (pH 7.4). Red blood cell contaminates were removed by Percoll (Sigma-Aldrich) gradient centrifugation (30% Percoll/Hanks basal salt solution containing 0.1% BSA without phenol red; pH 7.4) at 470 × *g* for 30 min (4°C). The granulosa cell (GC) fraction was then isolated and diluted 1:5 in Ham F-10/0.1% BSA medium to remove any contaminating Percoll. A final centrifugation was performed at 170 × *g* to pellet GCs; viability was assessed by trypan blue (Sigma-Aldrich) dye exclusion. Cells were cultured in fibronectin-coated 48-well plates (50 000–100 000 viable cells per well; 18 wells/aspiration) in DMEM/F12 medium containing 15 mM HEPES, 100 U penicillin/100 μg/ml streptomycin, ITS liquid media supplement, 0.028 mg/ml LDL, 0.002 mg/ml aprotinin, and 50 ng/ml FSH in a humidified incubator at 37°C/5% CO_2 [21]. One hour after plating, NLGCs were exposed to shPGR, shScram, or no virus for 24 h (3.9×10^7 PFU/ml; n = 6 wells/vector). Following 24 h incubation with vectors, 20 IU/ml hCG was added to half of the wells of each group to induce in vitro luteinization (LGCs). Media were changed and spent media collected and pooled per treatment at 48, 72, and 120 h postvector (24, 48, and 96 h post-hCG exposure), and processed for evaluation of medium P levels (n = 4 females/cell type/time point). Additionally, contents of one randomly chosen well from each cell type (hCG vs. no hCG) and vector were collected for RNA analyses as described below at the same time points (n = 4 females/cell type/time point). A subset of cells was plated on charcoal-treated fetal calf serum (HyClone media supplement; Thermo Scientific)-coated eight-well glass chamber slides (Nunc Inc.) and processed for immunocytochemical analysis of PGR protein expression 72 h post-vector exposure.

Experiment 2

Rhesus macaque females (n = 12) were monitored for initiation of menstruation to identify the beginning of the follicular phase (Cycle Day 1). Four to six days later (depending on length of previous menstrual cycle), serum E2 and P levels were monitored daily [22] and COv protocols were initiated when serum E2 levels reached 90–120 pg/ml, indicating selection of the dominant antral follicle (Supplemental Fig. S1 [Supplemental Data are available online at www.biolreprod.org]; see [22] for details of the rhesus macaque COv protocol). The morning after COv protocols were initiated, either shPGR or shScram vector (3.9×10^7 pfu/ml) was injected into the preovulatory follicle (n = 6 females/vector; [18]). The ovulatory hCG bolus was administered 20–22 h postintrafollicular injection, to ensure adequate production of shRNAs prior to the increase in *PGR* mRNA that typically occurs within 12 h post-hCG delivery [3, 23]. Ovaries were evaluated by laparoscopic methods for ovulation 96 h after intrafollicular vector injection, and several (n = 4/vector) were collected [23] for histological evaluation and immunohistochemistry to observe follicular morphology and PGR protein expression as described below. Daily serum samples were collected for E2 and P analyses throughout COv protocols until time of ovariectomy.

Real-Time PCR

Total RNA from NLGCs and LGCs (n = 4/cell type/time point/vector) from samples obtained in experiment 1 was extracted using Absolutely RNA Nanoprep Kit (Stratagene, Agilent Technologies) and reverse transcribed using High Capacity RNA-to-cDNA Kit (Life Technologies). TaqMan real-time PCR was performed by reported methods [24] using previously validated primer/probes specific for macaque *PGR* and the invariant housekeeping *MRPS10* mRNAs [25]. The potential PGR target genes steroidogenic acute regulatory protein (STAR) and HSD3B2 were analyzed in remaining RNA from samples (n = 3–4/cell type/time point/vector) by TaqMan real-time PCR using previously validated primers/probes [26].

Immunocytochemistry of PGR

Chamber slides containing NLGCs and LGCs from experiment 1 were rinsed with warm (37°C) PBS. Cells were then fixed at 37°C in 2% formalin/PBS for 15 min, rinsed again in PBS, and permeabilized with 0.2% Triton X in PBS for 5 min at room temperature. Following a final rinse with PBS, cells were incubated in Image-iT FX Signal Enhancer (Life Technologies) according to the manufacturer's protocols to reduce nonspecific interactions between the PGR antibody and macaque proteins. The cells were then incubated with rabbit anti-human PGR antibody (1:200 dilution; A0098; Dako) previously validated for use in macaque tissues [19] in PBS containing 1% BSA for 2 h at room temperature. After washing with PBS containing 0.1% Triton X, cells were incubated with Alexa Fluor secondary goat anti-rabbit IgG antibody (Alexa Fluor 594; Molecular Probes, Thermo Fisher Scientific) diluted in PBS/1% BSA as per the manufacturer's protocols. Lastly, after washing the slides with PBS/0.1% Triton X, cell nuclei were counterstained with 4′,6-diamidino-2-phenylindole (DAPI; Life Technologies) for 5 min at room temperature. After washing (PBS/1% BSA), coverslips were mounted on the slides using glycerol containing ProLong Antifade reagent (Life Technologies). Cells were imaged with an inverted microscope attached to a reflected light fluorescence laser with filters to both Texas red (PGR) and DAPI (nuclear contents). Images for each dye were obtained and merged using ImageJ software [27].

Ovaries from experiment 2 were processed for histology and immunocytochemistry as previously described [19]. Formalin-fixed ovaries were embedded in paraffin, 5-μm sections placed on glass permafrost slides, and selected sections processed for hematoxylin and eosin staining [19] to define tissue morphology. Other tissue sections were deparaffinized and processed for analysis of PGR protein using methods similar to previous studies [19] with anti-rabbit PGR antibody (1:100 dilution; A0098, Dako). Following incubation with the primary antibody, ovarian sections were incubated with biotinylated goat anti-rabbit IgG antibody and Vectastain ABC reagent according to the manufacturer's protocol (Vector Laboratories). Positive staining was detected by incubation of sections with 3,3′-diaminobenzidine (DAB reagent; Abcam) for ~5 min. All sections were processed with positive control tissue (CL) and negative control sections (omission of primary antibody) for each set of reactions.

Hormone Assays to Detect Steroids in Media and Serum Samples

Macaque serum samples were analyzed for E2 and P levels in the ONPRC Endocrine Technology Support Core Laboratory using a Roche Cobas e411 automatic clinical platform previously validated for detection of macaque steroids [28]. This platform included three internal controls per assay, and intra- and interassay coefficients of variation were consistently <7%. Lower limits of detection for E2 and P were 5 pg/ml and 0.035 ng/ml, respectively. P levels in medium samples obtained from granulosa cell cultures were also analyzed using the same platform.

Statistics

Real-time PCR, medium, and serum hormone sample data were analyzed by repeated-measures ANOVA (mixed model procedure of SAS, version 9.3, SAS Institute Inc.). For in vitro study, factors interrogated included time of collection, hCG exposure, and vector treatment. In vivo study factors included time from hCG exposure and vector treatment. Post hoc analyses of differences were interrogated by least squared means function of SAS (which controls for multiple comparisons) for preplanned comparisons. In vitro studies were analyzed by vector exposure within time period collected and CG exposure status (cell type). In vivo studies were analyzed by vector treatment exposure within time from hCG. All P values <0.05 were considered significant, and any between 0.06 and 0.08 were considered a trend.

RESULTS

Studies employing a vector consisting of a replication-incompetent adenovirus to induce expression of EGFP by transduced cells determined that a viral titer of 3.9×10^7 pfu/ml provided optimal transduction of macaque granulosa cells in vitro (Fig. 1, A and B, NLGC), regardless of prior in vivo hCG exposure (Fig. 1, C and D, LGC). Cellular toxicity was not observed at this viral titer (data not shown). Induction of EGFP expression in follicle cells of the dominant antral follicle was evident in situ by detection of EGFP luminescence from whole ovarian tissue following intrafollicular injection of EGFP vector (Fig. 1, E and F). In vivo experiments confirmed an estimated local titer of 3.9×10^7 pfu/ml within the follicular fluid of the antral follicle provided sufficient transduction of follicular cells with low toxicity (Fig. 1, G–I) as evident by ovarian cells with positive immunostaining for EGFP by 24 (Fig. 1G) and 72 h (Fig. 1H) post vector injection. Although there was some variability in efficiency of transduction at 24 h, all luteinizing granulosa cells showed high levels of EGFP expression 72 h postinjection. Therefore, all remaining experiments were conducted using this titer of adenovirus.

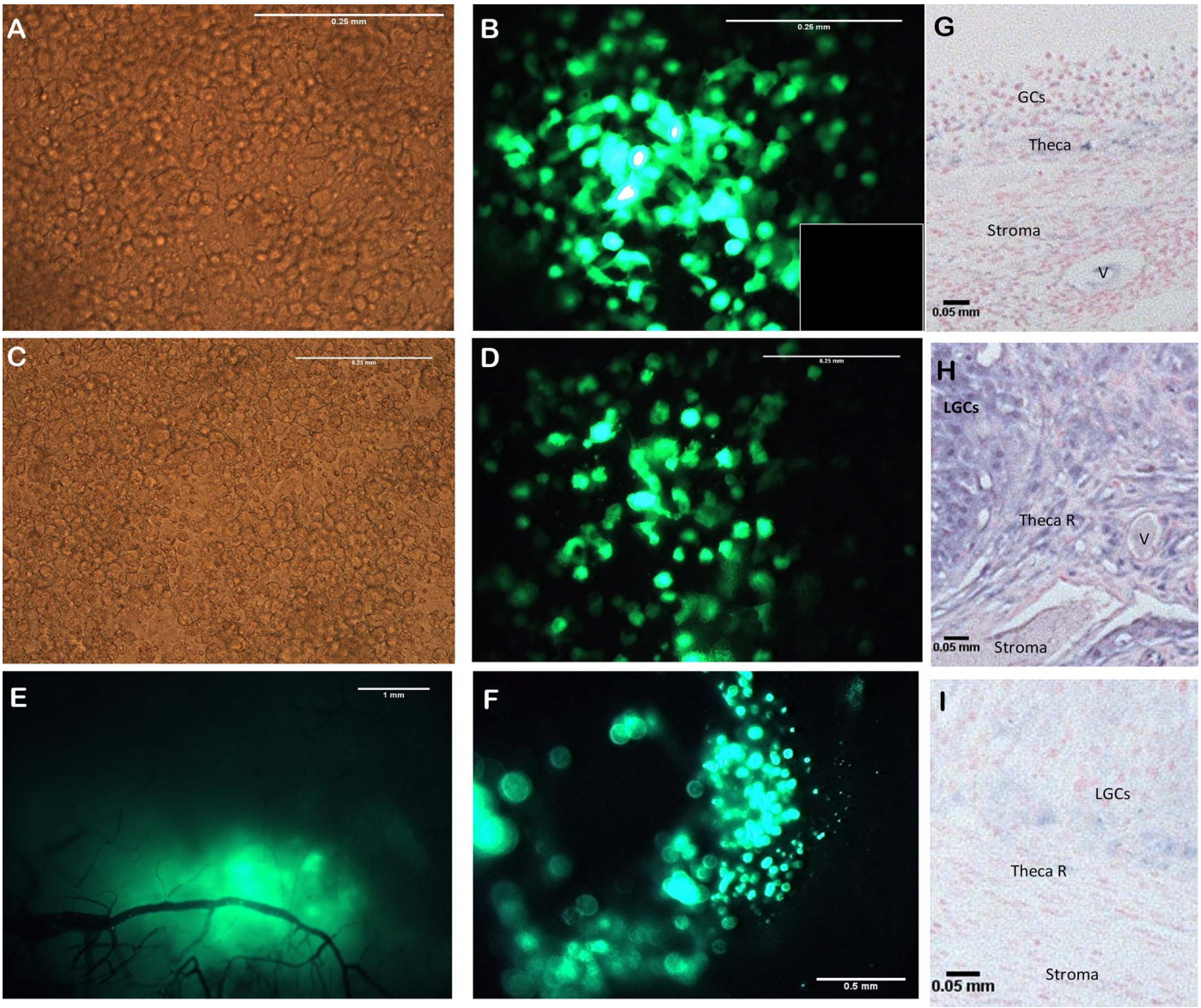

FIG. 1. A vector containing an expression cassette of the EGFP gene to induce GFP production by transduced cells was used to validate the ability of adenovirus to infect macaque granulosa cells in vitro (**A**–**D**) and in vivo (**E**–**H**). **A** and **B**) NLGCs were cultured and imaged 24 h after EGFP-vector exposure as described in *Materials and Methods*. **A** is a bright-field image; **B** is an image collected with a FITC filter. NLGCs not exposed to virus are depicted in white boxed inset in **B** (FITC filter). **C** and **D**) LGCs were cultured and imaged 24 h after EGFP-vector exposure as described in *Materials and Methods*. **C** is a bright-field image; **D** is an image collected with a FITC filter. **E**–**H**) Monkeys undergoing COv protocols (similar to Supplemental Fig. S1; see *Materials and Methods*) received an intrafollicular injection of EGFP vector, and the treated ovary was removed 72 h (**E** and **F**) after vector injection. **E** shows EGFP luminescence emitting through the outside wall of the ovulated follicle (imaged with FITC filter); **F** is a fluorescent image taken from the same ovary after cross-sectioning of the follicle. **G** and **H** depict follicular EGFP protein expression by immunohistochemistry 24 (**G**) and 72 h (**H**) following intrafollicular injection of EGFP vector (as detailed in *Materials and Methods*; purple staining indicates presence of EGFP protein). **I**) EGFP staining of an ovulated follicle collected 70 h post-hCG that was not injected with EGFP vector (negative control). GC, granulosa cell layer; Theca, theca cell layer; Theca R, remnant of theca cell layer; V, vessel; Stroma, adjacent ovarian stroma tissue. Bars = 0.25 mm (**A**–**D**), 1 mm (**E**), 0.5 mm (**F**), and 0.05 mm (**G**–**I**).

Experiment 1

In vitro luteinization following hCG treatment increased *PGR* mRNA levels in rhesus macaque GCs compared to controls (overall LGCs vs. NLGCs; $P < 0.003$). Exposure of NLGCs and LGCs to vector containing nontargeting scrambled control shRNA (shScram) had no significant effect on mRNA levels of *PGR* at any time point compared to no-virus controls (Fig. 2; $P > 0.4$). Treatment with vector containing shRNA targeted to *PGR* (shPGR) significantly reduced *PGR* mRNA levels by 44% in NLGCs within 48 h post-vector exposure compared to controls (no virus; $P < 0.001$), with a further reduction of 83% at 120 h ($P < 0.0002$). Treatment of LGCs with shPGR during in vitro luteinization significantly reduced *PGR* mRNA levels by 74% at 48 h post-hCG exposure (72 h postvector; $P < 0.0001$), with a maximum inhibition of 87% observed at 96 h post-hCG treatment (120 h postvector; $P < 0.0001$).

Expression of PGR protein, as judged by fluorescent immunostaining, is diffuse in shScram-exposed NLGCs, but becomes predominantly nuclear in LGCs at 48 h following hCG treatment (Supplemental Fig. S2, A and D). Decreased PGR protein is appreciable in NLGCs and nuclear localization of PGR protein in LGCs is absent following shPGR vector

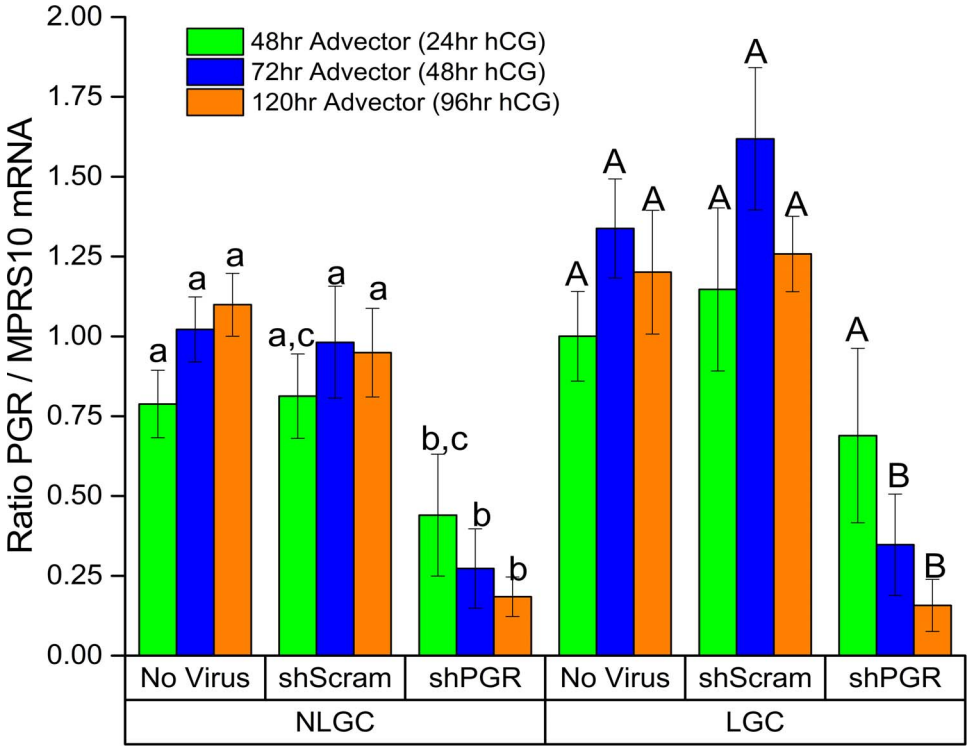

FIG. 2. Levels of *PGR* mRNA in NLGCs and in vitro luteinized GCs (LGCs) exposed to either no virus, shScram vector, or shPGR vector for up to 120 h of culture (see text for details of treatments). Different lowercase letters and different uppercase letters indicate significant ($P < 0.05$) differences in *PGR* mRNA levels between individual vector treatments in NLGCs and LGCs, respectively.

treatment at 48 h post-hCG exposure (Supplemental Fig. S2, B, C, E, and F).

There was no effect of shScram vector on medium P levels in NLGCs compared to no-virus controls (Fig. 3A, $P > 0.01$; only 120-h time point shown). Treatment of NLGCs with shPGR vector significantly reduced P levels at 120 h (Fig. 3A, $P < 0.03$). Increased P levels were observed in media of LGCs following hCG exposure in shScram vector-treated cells similar to no-virus controls at 96 h (120 h in culture; Fig. 3A; effect of hCG, $P < 0.0001$; effect of hCG as a function of time in culture, $P < 0.04$). Treatment with shPGR vector (120 h) also prevented the rise in P levels in LGCs at 96 h post-hCG, compared to no-virus control (Fig. 3A, $P < 0.01$). Overall, the ability of shPGR vector to significantly reduce both basal (NLGCs) and hCG-induced (LGCs) P production was observed following 120 h of culture (effect of shPGR vector, $P < 0.0001$; effect of shPGR vector as a function of time in culture, $P < 0.001$).

The mRNA of potential targets of *PGR* in NLGCs and LGCs that mediate P production in primate granulosa cells were evaluated in NLGCs and LGCs. The mRNA levels for *STAR* and *HSD3B2* were low in NLGCs, and although shPGR vector marginally decreased mRNA levels, this decline was insignificant ($P > 0.2$; Fig. 3, B and C). In contrast, the levels of *STAR* mRNA were increased in primate granulosa cells by CG exposure (LGCs; Fig. 3B, $P < 0.006$, only 120-h time point shown). Moreover, exposure to shPGR vector decreased *STAR* mRNA by 120 h of culture (Fig. 3B, $P < 0.04$). Similarly, the levels of *HSD3B2* mRNA were increased by exposure to CG in tandem with increased P production (Fig. 3C, $P < 0.03$, only 120 h time point shown). Exposure to shPGR vector also significantly reduced levels of *HSD3B2* in LGCs (Fig. 3C, $P < 0.001$).

Experiment 2

Because shPGR vector reduced *PGR* mRNA in vitro, we next sought to determine the effects of PGR knockdown in vivo. Intrafollicular injection of the shScram vector did not prevent ovulation and oocyte expulsion in six of six injected ovaries. By laparoscopic evaluation, the shScram-injected follicles typically displayed a rupture site, unless adhesions on the ovarian surface obstructed its view (example in Fig. 4A, arrow). Rupture sites were obvious by histology, with no evidence of a trapped oocyte within the luteinizing follicle/early CL in four of four shScram-injected follicles removed 72 h after an hCG bolus, even when the rupture site was obscured behind adhered tissue (Fig. 4E, arrow). In addition, immunostaining for PGR was evident in the luteinized cells, especially in the nucleus (Fig. 4, I and M), and follicles displayed morphology associated with granulosa cell hypertrophy and luteinization: granulosa cells streaming into the antrum and disappearance of the delineation between the theca and granulosa layers.

In contrast, injection of shPGR vector typically prevented ovulation and oocyte expulsion. Only one of six shPGR-injected follicles displayed a rupture site by laparoscopy (Fig. 4, B–D; blue arrow indicates rupture site). Upon removal of four ovaries at 72 h, only one of four follicles had a confirmed rupture site (Fig. 4D), and three of four follicles contained a trapped oocyte upon histologic evaluation (Fig. 4, F–H). These trapped oocytes were observed to be in the GV (not shown), metaphase I (MI; Fig. 4F), and metaphase II (MII; Fig. 4G) stages, indicating two of three had resumed meiotic processes. Notably, PGR immunostaining was low to absent in shPGR-exposed follicles at the time of ovariectomy (Fig. 4, J–L and N–P), regardless of ovulation status (PGR expression in the one ovulatory follicle depicted in Fig. 4, L and P). The mural

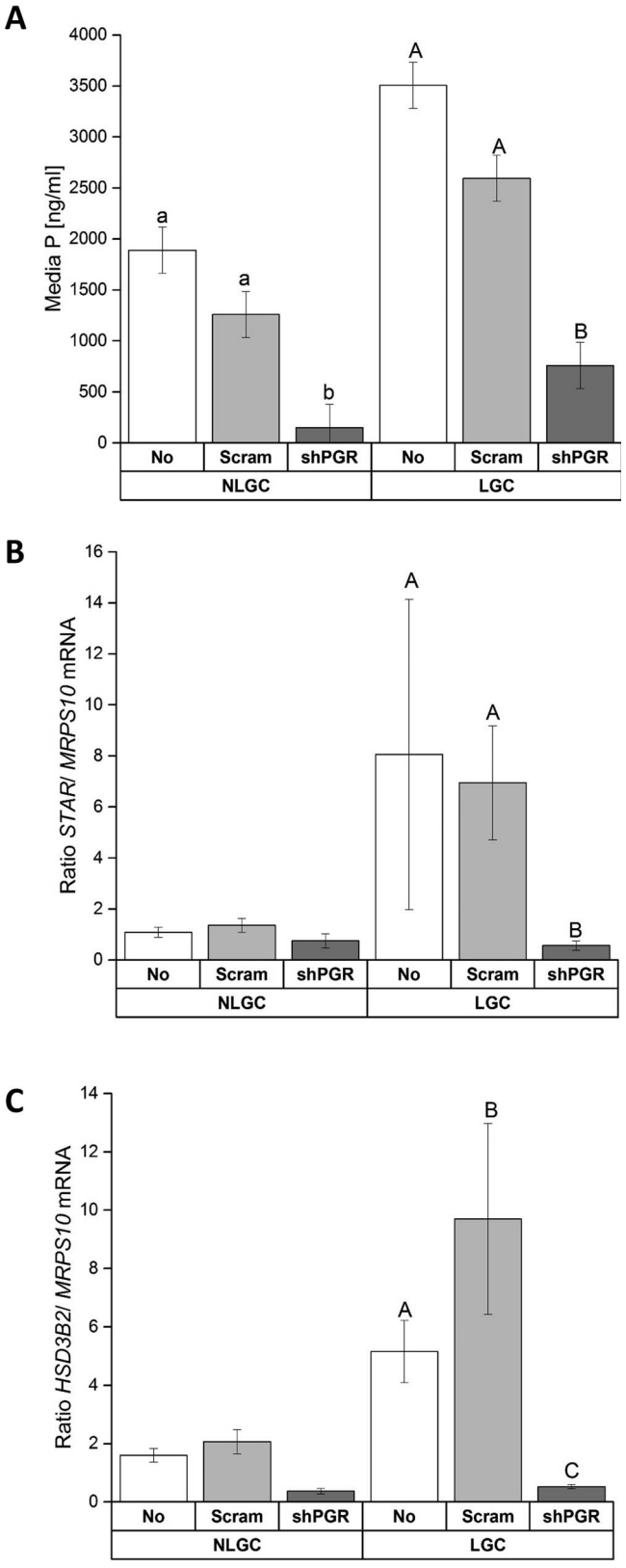

FIG. 3. Levels of medium P (**A**), *STAR* mRNA (**B**), and *HSD3B2* mRNA (**C**) from cultures of NLGCs and in vitro luteinized GCs (LGCs; +hCG) exposed to either no virus, shScram vector, or shPGR vector (see text for details of treatments) at 120 h of culture. Different lowercase and uppercase letters indicate significant ($P < 0.05$) differences in medium P levels between individual vector treatments in NLGCs and LGCs, respectively.

granulosa cells of shPGR-injected follicles exhibited a compact morphology and displayed few characteristics classically associated with ovulation and luteinization.

Serum levels of E2 were comparable before and after injection of follicles with shScram or shPGR vectors (Fig. 5A, $P > 0.7$); all females had similar peak E2 levels on the day of hCG administration (shScram 295 ± 56 pg/ml; shPGR 326 ± 62 pg/ml). Serum E2 levels declined following hCG administration (shScram 73 ± 21 pg/ml; shPGR 58 ± 10 pg/ml) and remained low until ovariectomy/evaluation (72 h). In contrast, serum P levels were significantly reduced in females receiving an intrafollicular injection of shPGR vector compared to those receiving shScram control (Fig. 5B, $P < 0.04$). Serum P levels of shScram control females increased to 0.9 ± 0.3 ng/ml by 72 h post-hCG, whereas P levels of shPGR females remained near pre-hCG levels at 0.3 ± 0.1 ng/ml ($P < 0.0002$).

DISCUSSION

Our initial data validate an RNAi approach to limit the expression of target genes and subsequent protein production in the primate ovary. Use of a replication-incompetent vector for shRNA delivery is particularly valuable for transient manipulation of gene function during discrete intervals, such as the periovulatory stage of the ovarian cycle. Unlike lentiviral delivery systems, the shRNA expression cassette delivered by vector is not incorporated into the host genome [29]. The limited expression interval of the shRNA, combined with the disappearance of the preovulatory follicle and subsequent CL at the end of the menstrual cycle, permits the repeated use of animals for control (shScram) and knockdown (shPGR) protocols, allowing at least one menstrual cycle of rest between experiments. Also, these vectors are highly efficient, thus requiring low titers of virus. By packaging the siRNA into longer shRNAs, immune responses associated with in vivo delivery of siRNAs may be minimized [30].

We also confirmed that the vector was capable of transducing ovarian (granulosa) cells for production of protein (e.g., EGFP) or inhibition of RNA (*PGR* mRNA). In vitro and in vivo studies demonstrated that relatively low (3.9×10^7 pfu/ml) viral titers generated appreciable levels of EGFP expression in granulosa cells with low toxicity. Moreover, this viral titer significantly reduced *PGR* mRNA levels by 74% at 48 h and up to 87% at 96 h post-hCG. This scale of reduction is superior to lipid-based transfection techniques, similar to previous reports [31] and personal experience with these vectors. The same shRNA targeting *PGR* only reduced mRNA levels by 60% when inserted into a plasmid and delivered via lipid-based transfection techniques under optimal conditions (data not shown). Finally, we demonstrated that the vector *PGR* shRNA delivery system results in loss of protein, as judged by immunocytochemistry to detect PGR in granulosa cells in vivo. The loss of PGR was particularly noticeable in the nucleus, where it resides in granulosa lutein cells after induction by an ovulatory dose of gonadotropin [32, 33]. Thus, this study, while specifically addressing the role P signaling plays via a nuclear receptor pathway in the ovulatory, luteinizing follicle, provides the basis for applying RNAi-based techniques to future studies on gene function in the primate ovary.

Notably, local delivery of shRNAs into a tissue can cause selective loss of gene function in cells or a tissue compartment of interest, e.g., the preovulatory follicle of the ovary. In our study, there was appreciable uptake of the vector from the follicular fluid into the granulosa cells of the injected preovulatory follicle, as judged by immunocytochemical staining for EGFP expression. Positive staining for EGFP in

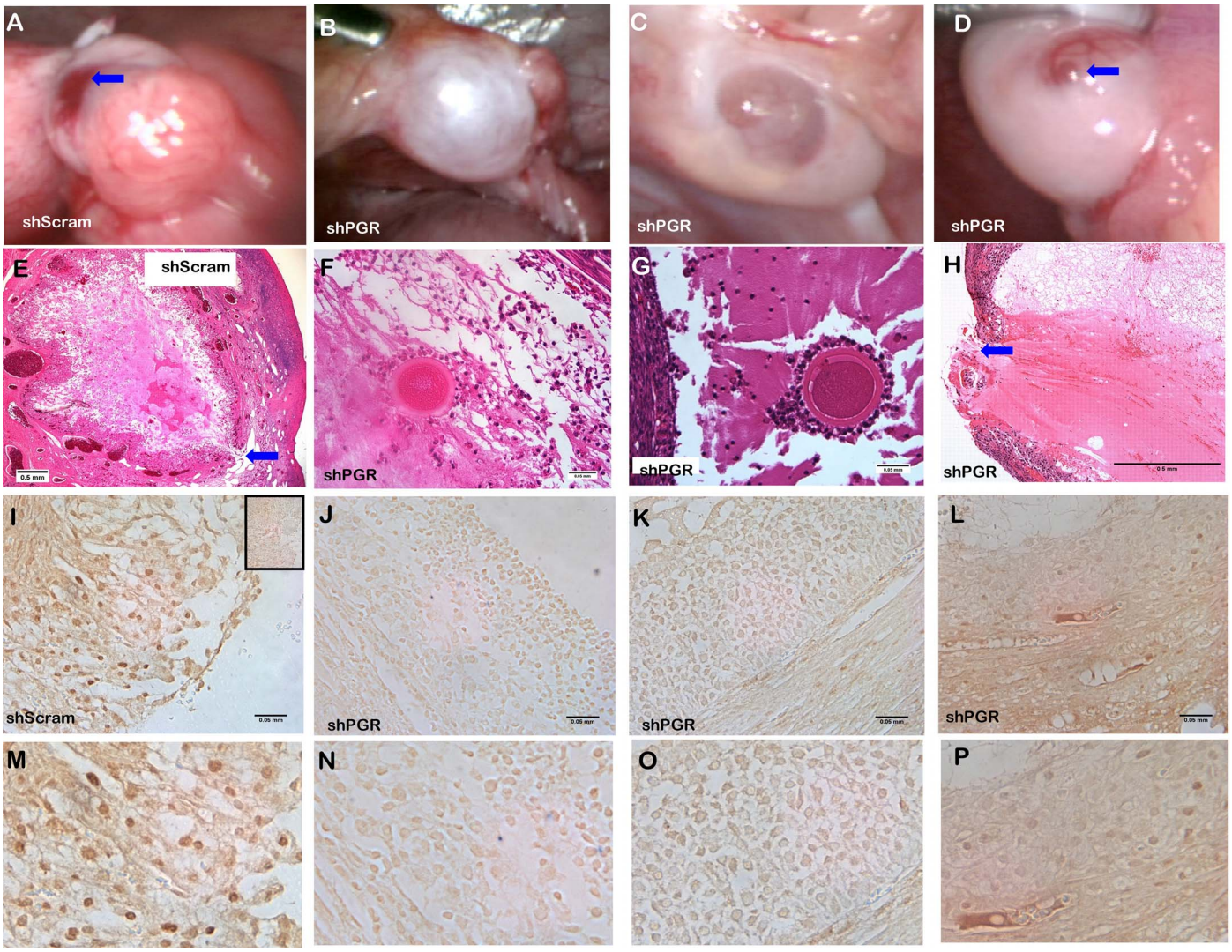

FIG. 4. Comparison of shScram vector (control; **A**, **E**, **I**, and **M**) and shPGR (**B**, **C**, **F**, **G**, **J**, **K**, **N**, and **O** are nonovulatory; **D**, **H**, **L**, and **P** depict the one ovulatory follicle) injected follicles at 72 h after an hCG bolus, approximately 36 h after the anticipated time of follicle rupture. **A**–**D**) Images obtained by laparoscopic evaluation (ovulation site indicated by blue arrow). **E**–**H**) Hematoxylin and eosin (H&E) evaluation of either the ovulation site (**E** and **H**, blue arrows) or a trapped oocyte in unruptured follicles (**F** and **G**). **I**–**L**) Images of PGR protein detection by immunohistochemistry (brown color indicates positive staining; no-primary-antibody negative control is included as an inset in **I**). **M**–**P**) Enlarged images of **I**–**L** to show granulosa cell morphology and PGR expression. The shScram-injected follicles typically displayed an ovulatory stigma upon laparoscopic evaluation (**A**, blue arrow). Another shScram-injected ovary, in which the ovulation site was masked by tissue adhesions, displays a rupture site and absence of a trapped oocyte after tissue sectioning (**E**, blue arrow). Nuclear immunostaining of PGR protein is present in LGCs as they fill the antrum and the follicle wall breaks down (**I** and **M**). Follicle rupture was not observed in five of six shPGR-injected follicles (nonovulatory follicles, **B** and **C**), and trapped oocytes were found in unruptured follicles after ovarian sectioning (**F** and **G**), indicating disruption of ovulatory process by shPGR vector. Oocytes trapped in follicles were observed to be in MI (**F**), MII (**G**), and GV-intact (not shown) stages. Follicle rupture was confirmed in only one shPGR-injected follicle as evidenced by small stigma upon laparoscopic evaluation (**D**, blue arrow) and clear rupture site by H&E tissue staining (**H**). However, regardless of ovulation status, loss of nuclear PGR protein was observed in all shPGR-injected follicles by immunocytochemistry (**I**–**L** and **M**–**P**; ovulation observed in follicle depicted in **L** and **P**). Bars = 0.5 mm (**E** and **H**) and 0.05 mm (**F**–**G**, **I**–**L**).

the theca cells and surrounding stromal cells, as well as granulosa cells in neighboring follicles, was also observed. It is unclear if thecal-stromal uptake occurred before or after dissolution of the basement membrane separating the granulosa and theca cell layers of the ovulatory follicle, or if uptake by extraneous follicles was associated with the path of the injection needle. Nevertheless, our results confirm that local delivery of adenoviral shRNA vector via injection into the antral follicle (current study), or by short-term infusion/injection into the cortex (Xu and Bishop, unpublished results) or CL [34], provides a means to manipulate gene function in compartments of the primate ovary. Moreover, by evaluating the time frame for shRNA inhibition of gene function and protein production, treatments can be coordinated with regulatory events in the ovary, such as the onset of an ovulatory gonadotropin surge. Thus, in the current study, the shRNA vector was injected into the preovulatory follicle ~22 h before administering the hCG bolus to allow time for granulosa cell transduction and sufficient *PGR* siRNA formation prior to and during the induction of *PGR* mRNA 12–36 h post-hCG [3, 23].

The use of a shRNA vector to deplete *PGR* mRNA and protein expression caused loss of function in granulosa cells in vitro and in the periovulatory follicle in vivo. First, intrafollicular injection of the *PGR* shRNA vector prevented ovulation, as judged laparoscopically by the absence of

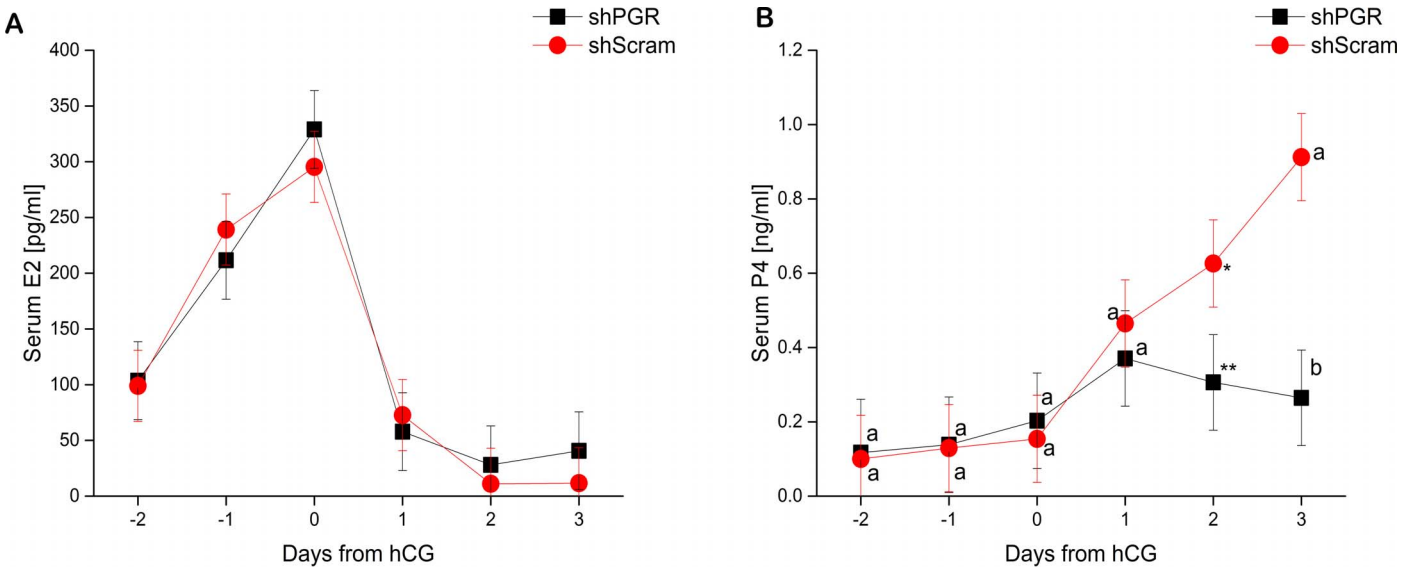

FIG. 5. Serum E2 (**A**) and P (**B**) levels in rhesus macaque females undergoing COv protocols receiving intrafollicular injection of vectors shPGR or shScram. The day of intrafollicular injection is indicated on graph (arrow). There were no significant effects of shPGR vector on timing, duration, or absolute level of serum E2 response to ovulatory hCG bolus ($P > 0.07$). Different lowercase letters indicate significant differences between P levels between vectors on individual sample days ($P < 0.05$). Asterisks indicate trend towards differences between vectors by day ($P < 0.06$).

ovulatory stigmata, in all but one monkey. The injection of adenovirus expressing a scrambled control shRNA, however, had no effect on timely ovulation. Moreover, when the ovary bearing the injected follicle was removed from four animals, serial sections confirmed the absence of a ruptured apex and the presence of a trapped oocyte in all ovaries but the one deemed ovulatory at laparoscopy. These results are consistent with our previous study wherein pharmacologic blockade of P production prevented ovulation of multiple follicles during COS cycles in monkeys [5]. By using a COv protocol, which permits development of the naturally selected dominant follicle, we confirm that P's ovulatory action in the primate ovary is likely mediated via the classic nuclear PGR. Notably, immunocytochemical analyses at 72 h post-hCG indicated that PGR was markedly suppressed in all follicles receiving the shPGR vector. This time point is well beyond when timely ovulation (36–38 h post-hCG [22]) occurs. One follicle did rupture that received shPGR adenovirus, although it is unclear if for some reason the PGR expression level in this follicle was not reduced sufficiently to prevent the cascade of events leading to ovulation. Alternatively, nonclassical P receptors such as *PGRMC1* [35] or members of the class II progestin and adipoQ receptor (*PAQR*) family [36] may partially compensate for the nuclear P receptor, leading to an occasional ovulation. Our studies cannot distinguish between the actions of *PGR-A* and *-B* isoforms. Previous experiments in the mouse demonstrated that *Pgr-a*, not *Pgr-b*, is critical for P-mediated ovulation [37]. Because *PGR-A* and *-B* are encoded by a single gene, and *PGR-A* is a truncated isoform, it is not possible to selectively knockdown *PGR-A* using RNAi technology. However, alternative approaches may become feasible in the future, e.g., genetic manipulation using CRISPR/Cas9 or TALENs [38], that provide more targeted knockdown of genes in primate models.

Treatment with *PGR* shRNA in vitro or in vivo also markedly suppressed P production by the granulosa cells and the periovulatory follicle, respectively. This did not appear to be due to cellular toxicity, because the cultured cells exposed to shScram and shPGR yielded comparable amounts of total RNA at the time points investigated, i.e., cellular breakdown did not occur (data not shown). Furthermore, serum E2 levels remained comparable between treatments following follicular injection, whereas P levels remained near baseline in only the shPGR-injected females after the hCG bolus. A recent report of siRNA-mediated P-receptor (*PGR*, *PGRMC1*, and *PAQR*) depletion in a human luteinized granulosa cell line did not observe an effect of *PGR* siRNA on P production by these cells [39]; however, the cultures were assayed at 48 h post-siRNA transfection. Our data indicate that this time point is too early to observe any effects on either LH/CG-stimulated or basal P synthesis by granulosa cells. If ovulatory processes are tied to P production by the ovarian cells, the long duration (120 h) needed to observe the effect of *PGR* knockdown on P production in vitro suggests these processes are mediated by the *PGR* acting as a transcription factor in the nucleus of the granulosa cell [40].

Notably, *PGR* depletion in luteinizing granulosa cells significantly reduced the mRNA levels for *STAR* (steroidogenic acute regulatory protein) and *HSD3B2* (enzyme converting pregnenolone to P) in a time-dependent manner. This suppression is similar to that observed during our previous studies on rhesus monkeys where steroid depletion in vivo decreased *STAR* mRNA in 1) granulosa cells of preovulatory follicles within 12 h of hCG administration in ovarian stimulation cycles [41] and 2) the functional CL of the menstrual cycle [25]. Moreover, when tested in the latter scenario, progestin replacement prevented the significant decline in *STAR* mRNA and protein [25]. In contrast, a decline in *HSD3B2* mRNA levels was not observed in these studies. Our data support the concept that P-PGR signaling directly promotes P synthesis in luteinizing granulosa and luteal cells by stimulating a key component in the steroidogenic process, STAR. Moreover, at the time of luteal development, P-PGR signaling may also promote P production by inducing expression of HSD3B2. Our data further support the hypothesis introduced by Rothchild [42] that P promotes its own synthesis in the developing CL, and provide evidence suggesting this action is mediated by nuclear PGR signaling pathways. Alternatively, promotion of P synthesis by P-PGR signaling may be part of a more global action to promote luteinizing

processes within the macaque CL. These results differ from those in PRKO/PRAKO mice, wherein initial luteinization and markers of steroidogenesis following equine chorionic gonadotropin-hCG treatment were comparable to those of wild-type mice [43]. Given the species-specific differences in other ovulatory processes between primates and rodents [10], further primate studies using these shScram and shPGR vectors are necessary to clarify the role of P-PGR signaling in promoting steroidogenesis and luteal development in primates.

The identification of additional periovulatory processes regulated by P or P signaling is an area of active investigation. Previous studies in rhesus monkeys during COS cycles [44] revealed that several members of the metalloproteinase (MMP) family of enzymes are dynamically expressed in ovulatory, luteinizing follicles, with the expression of the collagenase MMP1 being induced by P. Studies with *Pgr-a* mutant (PRAKO) mouse model identified a disintegrin and metalloproteinase with thrombospondin-like repeats (*Adamts*)-1 and *cathepsin L* as likely P-regulated genes in the cascade leading to tissue dissolution and follicle rupture [45]. It appears that MMP/ADAMTS family members are important for ovulation; intrafollicular injection of a broad inhibitor of the MMP family significantly reduced ovulation during COv cycles in monkeys [46]. Recent analyses of the transcriptome in periovulatory follicles identified mRNAs for 10 proteases that might be involved in the tissue reorganizing required for ovulation and/or luteal development [46], with the most likely candidate MMP1. Further investigation employing the shPGR and shScram vectors will help delineate the gene products and cellular pathways whereby P-PGR signaling promotes ovulation in primates.

In summary, these data support a direct role for P to induce ovulatory processes via PGR signaling in primates. Additionally, as hypothesized by Rothchild [42], P regulates its own biosynthesis in luteinizing granulosa cells both before and immediately after ovulation. Further studies employing these shRNA vectors should reveal specific gene processes disrupted by PGR silencing and elucidate the specific pathways induced or inhibited by PGR in primate granulosa-lutein cells. Because two of the three trapped oocytes reinitiated meiosis, oocyte maturation may not be regulated directly by P via PGR; this observation is consistent with previous studies on rhesus macaques administered an antiprogestin during COS cycles [47]. Finally, these studies provide the basis for additional knockdown studies employing shRNA vectors targeting other local factors or their receptors to better understand the control of ovarian function in nonhuman primates.

ACKNOWLEDGMENT

The authors are grateful to the contributions of the ONPRC DCM, especially the SSU under the direction of Dr. Theodore Hobbs, for their expertise in assisting all studies involving nonhuman primates reported here. The authors are also indebted to the contributions of the ONPRC Endocrine Technology Services Laboratory, under Directors Dr. Francis Pau (Ret.) and Dr. David Erickson, for conducting all Roche assays. We thank Dr. Carol Hanna for assistance with staging oocytes present in H&E sections. These experiments benefited from the years of expertise of Dr. Theodore Molskness (Ret.) in the field of primate reproductive physiology. Finally, the authors thank Jeffrey Torgerson and the ONPRC Molecular Virology Support Core for generation of all adenoviral products.

REFERENCES

1. Chaffin CL, Stouffer RL. Role of gonadotrophins and progesterone in the regulation of morphological remodelling and atresia in the monkey periovulatory follicle. Hum Reprod 2000; 15:2489–2495.
2. Chaffin CL, Hess DL, Stouffer RL. Dynamics of periovulatory steroidogenesis in the rhesus monkey follicle after ovarian stimulation. Hum Reprod 1999; 14:642–649.
3. Chaffin CL, Stouffer RL, Duffy DM. Gonadotropin and steroid regulation of steroid receptor and aryl hydrocarbon receptor messenger ribonucleic acid in macaque granulosa cells during the periovulatory interval. Endocrinology 1999; 140:4753–4760.
4. Elassar A, Liu X, Scranton V, Wu CA, Peluso JJ. The relationship between follicle development and progesterone receptor membrane component-1 expression in women undergoing in vitro fertilization. Fertil Steril 2012; 97:572–578.
5. Hibbert ML, Stouffer RL, Wolf DP, Zelinski-Wooten MB. Midcycle administration of a progesterone synthesis inhibitor prevents ovulation in primates. Proc Natl Acad Sci U S A 1996; 93:1897–1901.
6. Hill KK, Roemer SC, Churchill ME, Edwards DP. Structural and functional analysis of domains of the progesterone receptor. Mol Cell Endocrinol 2012; 348:418–429.
7. Hashimoto-Partyka MK, Lydon JP, Iruela-Arispe ML. Generation of a mouse for conditional excision of progesterone receptor. Genesis 2006; 44:391–395.
8. Couse J, Hewitt S, Korach K. Steroid receptors in the ovary and uterus. In: Neill JD, Plant TM, Pfaff DW, Challis JRG, de Kretser DM, Richards JS, Wassarman PM, (eds). Knobil and Neill: Physiology of Reproduction, 3rd ed. New York: Academic Press; 2006:593–678.
9. Chaffin CL, Stouffer RL. Local role of progesterone in the ovary during the periovulatory interval. Rev Endocr Metab Disord 2002; 3:65–72.
10. Chaffin CL, Vandevoort CA. Follicle growth, ovulation, and luteal formation in primates and rodents: a comparative perspective. Exp Biol Med (Maywood) 2013; 238:539–548.
11. Kumar LD, Clarke AR. Gene manipulation through the use of small interfering RNA (siRNA): from in vitro to in vivo applications. Adv Drug Deliv Rev 2007; 59:87–100.
12. Shen C, Buck AK, Liu X, Winkler M, Reske SN. Gene silencing by adenovirus-delivered siRNA. FEBS Lett 2003; 539:111–114.
13. Sitzmann BD, Leone EH, Mattison JA, Ingram DK, Roth GS, Urbanski HF, Zelinski MB, Ottinger MA. Effects of moderate calorie restriction on testosterone production and semen characteristics in young rhesus macaques (*Macaca mulatta*). Biol Reprod 2010; 83:635–640.
14. Peng HH, Wu S, Davis JJ, Wang L, Roth JA, Marini FC, Fang B. A rapid and efficient method for purification of recombinant adenovirus with arginine–glycine–aspartic acid-modified fibers. Anal Biochem 2006; 354: 140–147.
15. Anderson R, Haskell R, Xia H, Roessler B, Davidson B. A simple method for the rapid generation of recombinant adenovirus vectors. Gene Ther 2000; 7:1034–1038.
16. Hanna CB, Yao S, Ramsey CM, Hennebold JD, Zelinski MB, Jensen JT. Phosphodiesterase 3 (PDE3) inhibition with cilostazol does not block in vivo oocyte maturation in rhesus macaques (*Macaca mulatta*). Contraception 2015; 91:418–422.
17. Duffy DM, Molskness TA, Stouffer RL. Progesterone receptor messenger ribonucleic acid and protein in luteinized granulosa cells of rhesus monkeys are regulated in vitro by gonadotropins and steroids. Biol Reprod 1996; 54:888–895.
18. Hazzard TM, Rohan RM, Molskness TA, Fanton JW, D'Amato RJ, Stouffer RL. Injection of antiangiogenic agents into the macaque preovulatory follicle: disruption of corpus luteum development and function. Endocrine 2002; 17:199–206.
19. Wright JW, Jurevic L, Stouffer RL. Dynamics of the primate ovarian surface epithelium during the ovulatory menstrual cycle. Hum Reprod 2011; 26:1408–1421.
20. Wolf DP, Vandevoort CA, Meyer-Haas GR, Zelinski-Wooten MB, Hess DL, Baughman WL, Stouffer RL. In vitro fertilization and embryo transfer in the rhesus monkey. Biol Reprod 1989; 41:335–346.
21. Duffy DM, Stouffer RL. Luteinizing hormone acts directly at granulosa cells to stimulate periovulatory processes: modulation of luteinizing hormone effects by prostaglandins. Endocrine 2003; 22:249–256.
22. Young KA, Chaffin CL, Molskness TA, Stouffer RL. Controlled ovulation of the dominant follicle: a critical role for LH in the late follicular phase of the menstrual cycle. Hum Reprod 2003; 18:2257–2263.
23. Xu F, Stouffer RL, Muller J, Hennebold JD, Wright JW, Bahar A, Leder G, Peters M, Thorne M, Sims M, Wintermantel T, Lindenthal B. Dynamics of the transcriptome in the primate ovulatory follicle. Mol Hum Reprod 2011; 17:152–165.
24. Bishop CV, Aazzerah RA, Quennoz LM, Hennebold JD, Stouffer RL. Effects of steroid ablation and progestin replacement on the transcriptome of the primate corpus luteum during simulated early pregnancy. Mol Hum Reprod 2014; 20:222–234.
25. Bishop CV, Hennebold JD, Stouffer RL. The effects of luteinizing

hormone ablation/replacement versus steroid ablation/replacement on gene expression in the primate corpus luteum. Mol Hum Reprod 2009; 15: 181–193.
26. Bishop CV, Satterwhite S, Xu L, Hennebold JD, Stouffer RL. Microarray analysis of the primate luteal transcriptome during chorionic gonadotrophin administration simulating early pregnancy. Mol Hum Reprod 2011; 18:216–227.
27. Abramoff MD, Magelhaes PJ, Ram SJ. Image processing with ImageJ. Biophotonics Int 2004; 11:36–42.
28. Varlamov O, White AE, Carroll JM, Bethea CL, Reddy A, Slayden O, O'Rourke RW, Roberts CT Jr. Androgen effects on adipose tissue architecture and function in nonhuman primates. Endocrinology 2012; 153:3100–3110.
29. Hermens WT, Verhaagen J. Viral vectors, tools for gene transfer in the nervous system. Prog Neurobiol 1998; 55:399–432.
30. Couto LB, High KA. Viral vector-mediated RNA interference. Curr Opin Pharmacol 2010; 10:534–542.
31. Djurovic S, Iversen N, Jeansson S, Hoover F, Christensen G. Comparison of nonviral transfection and adeno-associated viral transduction on cardiomyocytes. Mol Biotechnol 2004; 28:21–31.
32. Wissing ML, Kristensen SG, Andersen CY, Mikkelsen AL, Host T, Borup R, Grondahl ML. Identification of new ovulation-related genes in humans by comparing the transcriptome of granulosa cells before and after ovulation triggering in the same controlled ovarian stimulation cycle. Hum Reprod 2014; 29:997–1010.
33. Hild-Petito S, Stouffer RL, Brenner RM. Immunocytochemical localization of estradiol and progesterone receptors in the monkey ovary throughout the menstrual cycle. Endocrinology 1988; 123:2896–2905.
34. Stouffer RL, Dahl KD, Hess DL, Woodruff TK, Mather JP, Molskness TA. Systemic and intraluteal infusion of inhibin A or activin A in rhesus monkeys during the luteal phase of the menstrual cycle. Biol Reprod 1994; 50:888–895.
35. Peluso JJ, Liu X, Gawkowska A, Johnston-MacAnanny E. Progesterone activates a progesterone receptor membrane component 1-dependent mechanism that promotes human granulosa/luteal cell survival but not progesterone secretion. J Clin Endocrinol Metab 2009; 94:2644–2649.
36. Petersen S, Intlekofer K, Moura-Conlon P, Brewer D, Pino Sans J, Lopez J. Nonclassical progesterone signalling molecules in the nervous system. J Neuroendocrinol 2013; 25:991–1001.
37. Richards JS, Russell DL, Ochsner S, Hsieh M, Doyle KH, Falender AE, Lo YK, Sharma SC. Novel signaling pathways that control ovarian follicular development, ovulation, and luteinization. Recent Prog Horm Res 2002; 57:195–220.
38. Gaj T, Gersbach CA, Barbas CF. ZFN, TALEN, and CRISPR/Cas-based methods for genome engineering. Trends Biotechnol 2013; 31:397–405.
39. Sueldo C, Liu X, Peluso JJ. Progestin and adipoQ receptor 7, progesterone membrane receptor component 1 (PGRMC1) and PGRMC2 and their role in regulating progesterone's ability to suppress human granulosa/luteal cells from entering into the cell cycle. Biol Reprod 2015; 93:63.
40. Lösel R, Wehling M. Nongenomic actions of steroid hormones. Nat Rev Mol Cell Biol 2003; 4:46–55.
41. Chaffin CL, Dissen GA, Stouffer RL. Hormonal regulation of steroidogenic enzyme expression in granulosa cells during the peri-ovulatory interval in monkeys. Mol Hum Reprod 2000; 6:11–18.
42. Rothchild I. The corpus luteum revisited: are the paradoxical effects of RU486 a clue to how progesterone stimulates its own secretion? Biol Reprod 1996; 55:1–4.
43. Robker RL, Russell DL, Espey LL, Lydon JP, O'Malley BW, Richards JS. Progesterone-regulated genes in the ovulation process: ADAMTS-1 and cathepsin L proteases. Proc Natl Acad Sci U S A 2000; 97:4689–4694.
44. Chaffin CL, Stouffer RL. Expression of matrix metalloproteinases and their tissue inhibitor messenger ribonucleic acids in macaque periovulatory granulosa cells: time course and steroid regulation. Biol Reprod 1999; 61: 14–21.
45. Robker RL, Russell DL, Yoshioka S, Sharma SC, Lydon JP, O'Malley BW, Espey LL, Richards JS. Ovulation: a multi-gene, multi-step process. Steroids 2000; 65:559–570.
46. Peluffo MC, Murphy MJ, Talcott Baughman S, Stouffer RL, Hennebold JD. Systematic analysis of protease gene expression in the rhesus macaque ovulatory follicle: metalloproteinase involvement in follicle rupture. Endocrinology 2011; 152:3963–3974.
47. Borman SM, Chwalisz K, Stouffer RL, Zelinski-Wooten MB. Chronic low-dose antiprogestin impairs preimplantation embryogenesis, but not oocyte nuclear maturation or fertilization in rhesus monkeys. Steroids 2003; 68:1041–1051.